

Absolute levels of transcripts for mitochondrial uncoupling proteins UCP2, UCP3, UCP4, and UCP5 show different patterns in rat and mice tissues

Lukáš Alán · Katarína Smolková · Eva Kronusová ·
Jitka Šantorová · Petr Ježek

Received: 7 November 2008 / Accepted: 29 January 2009 / Published online: 26 February 2009
© Springer Science + Business Media, LLC 2009

Abstract Existing controversies led us to analyze absolute mRNA levels of mitochondrial uncoupling proteins (UCP1–UCP5). Individual UCP isoform mRNA levels varied by up to four orders of magnitude in rat and mouse tissues. UCP2 mRNA content was relatively high (0.4 to 0.8 pg per 10 ng of total mRNA) in rat spleen, rat and mouse lung, and rat heart. Levels of the same order of magnitude were found for UCP3 mRNA in rat and mouse skeletal muscle, for UCP4 and UCP5 mRNA in mouse brain, and for UCP2 and UCP5 mRNA in mouse white adipose tissue. Significant differences in pattern were found for rat vs. mouse tissues, such as the dominance of UCP3/UCP5 vs. UCP2 transcript in mouse heart and vice versa in rat heart; or UCP2 (UCP5) dominance in rat brain contrary to 10-fold higher UCP4 and UCP5 dominance in mouse brain. We predict high antioxidant/antiapoptotic UCP function in tissues with higher UCP mRNA content.

Keywords Mitochondrial uncoupling proteins · UCP2 · UCP3 · UCP4 · UCP5 · Absolute mRNA levels

Introduction

With the exception of mitochondrial uncoupling protein 1 (UCP1), controversies in the research on UCPs cover all aspects including their putative function, i.e. doubts exist whether these proteins really uncouple mitochondria (Affourtit et al. 2007; Cannon et al. 2006; Esteves and Brand 2005). Their physiological roles in tissues will be undoubtedly given by the extent of uncoupling they induce when activated (Esteves and Brand 2005; Ježek et al. 2004). The lack of consensus on UCP function, even after a decade of research since the discovery of UCP2 and UCP3 isoforms, stems from the rather minute amounts expressed (with exception of UCP1) and imported into the inner membrane and from the lack of a clear understanding of isoform-specific tissue distribution. From a bioinformatics viewpoint, UCP1, UCP2, UCP3, UCP4, and UCP5 form a distinct subfamily within the gene family of mitochondrial anion carriers (Hanák and Ježek 2001; Ježek and Ježek 2003; Ježek and Urbánková 2000; Klingenspor et al. 2008). The carrier most sequentially similar to UCPs is the oxoglutarate carrier, which, however, lacks the unique uncoupling protein signature sequences (Hanák and Ježek 2001; Ježek and Ježek 2003; Ježek and Urbánková 2000). Functionally, *in vivo* uncoupling was demonstrated unequivocally for the first known member, UCP1, originally considered to be specific for brown adipose tissue (BAT), where it serves as the final molecular component of catabolic cascade of nonshivering thermogenesis (Cannon et al. 2006). However, UCP1 has also been detected in thymocytes (Adams et al. 2008a, b; Carroll et al. 2005),

Lukáš Alán and Katarína Smolková contributed equally to this work.

L. Alán · K. Smolková · E. Kronusová · J. Šantorová · P. Ježek
Department of Membrane Transport Biophysics, No.75, Institute
of Physiology, Academy of Sciences of the Czech Republic,
Prague, Czech Republic

L. Alán
e-mail: alan@biomed.cas.cz

K. Smolková
e-mail: smolkova@biomed.cas.cz

J. Šantorová
e-mail: santor@biomed.cas.cz

P. Ježek (✉)
Dept. No.75, Membrane Transport Biophysics,
Institute of Physiology, Academy of Sciences
of the Czech Republic, Vídeňská 1083,
14220 Prague 4, Czech Republic
e-mail: jezek@biomed.cas.cz

where its thermogenic role is probably replaced by a regulatory role in apoptosis due to its ability to attenuate production of mitochondrial reactive oxygen species (ROS) (Dlasková et al. 2006). ROS facilitate apoptosis, and hence UCP1 activation would have a preventive effect on apoptosis whereas UCP1 inhibition would promote apoptosis. UCP1 was recently detected in skin (Mori et al. 2008), where it is proposed to function (as in thymocytes) as a suppressor of mitochondrial ROS production.

Attempts to derive physiological roles for distinct UCPs also have been based on their expression pattern in various tissues. Owing to their low expression levels (with the exception of UCP1 in BAT), their thermogenic function is rather excluded and as the most relevant function seems to be the attenuation of mitochondrial ROS production (Affourtit et al. 2007; Arsenijevic et al. 2000; Cannon et al. 2006; Esteves and Brand, 2005; Jabůrek et al. 2004; Ježek et al. 2004). Indeed the mild uncoupling is able to attenuate both superoxide formation within Complex III (Ježek and Hlavatá, 2005) as well as Complex I (Dlasková et al. 2008a, b). The extent of such an “antioxidant” mechanism *in vivo* would depend not only on absolute UCP levels but also on the activation state of each UCP and the extent of inhibition by purine nucleotides (Beck et al. 2007). The absolute protein levels serve as a basic parameter for rough estimation of UCP functional relevance in a given tissue.

Determination of UCP expression patterns is difficult due to their extreme hydrophobicity and impossibility to raise antibodies, which would not cross-react with other UCPs (Pecqueur et al. 2001) or with other members of the anion carrier gene family. Hence, most studies have relied on methods quantifying UCP mRNA levels such as northern blotting and RT-PCR. Despite the translational down-regulation described for UCP2 (Hurtaud et al. 2006; Pecqueur et al. 2001) and UCP5 (Kim-Han et al. 2001), or the translational up-regulation of UCPs (Hurtaud et al. 2007), the precise determination of transcript levels still provides valuable information.

UCP2 is considered to be expressed ubiquitously in mammalian tissues (Fleury et al. 1997; Gimeno et al. 1997; Lengacher et al. 2004). In contrast, UCP3 mRNA has been detected in northern blots of human skeletal muscle and in rodent skeletal muscle, heart, and BAT (Boss et al. 1997; Vidal-Puig et al. 1997). The original reports for UCP5 and UCP4 mentioned their high expression in the central nervous system (Mao et al. 1999; Sanchis et al. 1998). Northern blotting also detected UCP5 mRNA in both mouse and human heart, kidney (Kim-Han et al. 2001; Sanchis et al. 1998; Yu et al. 2000) and skeletal muscle (Lengacher et al. 2004; Sanchis et al. 1998; Yu et al. 2000). These results were confirmed by UCP5 immunodetection (Kim-Han et al. 2001). However, Sanchis et al. (1998)

found even wider distribution of UCP5 mRNA, in the rat, mouse, and human gut, lung, testis, uterus, spleen, and white and brown adipose tissue. Additional findings were reported for the human prostate, pancreas, adrenal medulla and cortex, thyroid gland and liver, as well as for the mouse liver (but not spleen), lung, and skeletal muscle (Yu et al. 2000). Using quantitative RT-PCR with TaqMan probes, Lengacher et al. (2004) found not only UCP4 and UCP5 mRNA in the mouse brain cortex (together with a lower amount of UCP2 transcript), but also ~100 times lower levels of UCP3 and UCP1 mRNA. In BAT and skeletal muscle, Lengacher et al. (2004) also identified all five UCP mRNAs, with the UCP1 mRNA level in BAT being ~100-fold higher than all other isoforms, and with UCP3 mRNA level being at least 10-fold higher in skeletal muscle. It is unclear, however, whether the minute levels of UCP mRNAs become translated into mature proteins. If indeed they are translated, one must re-evaluate the molecular physiology of UCPs based on their tissue distribution in light of findings such as UCP1 mRNA in human pancreatic β -cells (Sale et al. 2007), UCP5 in endocrine cells (Ho et al. 2005, 2006), UCP4 mRNA in preadipocytes (Zhang et al. 2006), or of the emerging role of UCP4 and UCP5 in brain pathologies (Liu et al. 2006; Chan et al. 2006; Nakase et al. 2007; Naudí et al. 2007).

In this work, we used quantitative real-time RT-PCR to determine absolute levels of UCP mRNAs, except of UCP1, in selected tissues. The levels of different UCP mRNAs varied by up to four orders of magnitude in various rat tissues. Their distinct pattern was found in mouse tissues. Functional redundancy among UCPs was suggested by different dominance of certain isoforms in given rat and mouse tissues. Whereas UCP2 dominance was found in rat heart, UCP3 and UCP5 dominated in mouse heart. Similar UCP2 (UCP5) dominance in rat brain contrasted to UCP4 and UCP5 dominance in mouse brain with one order of magnitude higher levels of mRNAs.

Materials and methods

mRNA isolation

The total RNA was isolated from rat (Wistar, 250 to 275 g) and mouse (Balb/C, 20–25 g) tissues by a standard procedure (Chomczynski and Sacchi 1987). An RNase-free DNase-I was purchased from Top-Bio (Czech Republic). Routinely, mRNA was isolated from the DNase-I-treated total RNA, except for skeletal muscle and white adipose tissue (WAT), using an mRNA isolation kit (Roche Applied Science, USA) and Oligo(dT) 3'Bio-oligo(dT)₂₀ (Metabion, Czech Republic). Skeletal muscle and WAT mRNAs were extracted using a Fibrous Tissue and Regular Midi RNeasy

kit (Qiagen), respectively, including on-column DNase treatment. The samples of total RNA and mRNA were quantified from their spectra with a subtracted light scattering contribution using an Agilent 8453E UV-VIS spectroscopy system and 200- μ l quartz cuvettes. An mRNA sample was used for further analysis only when its purity was reflected by the A_{260}/A_{280} ratios of 1.7 to 1.9.

Design of primers and probes for real-time RT-PCR

We quantified UCP mRNAs using a reliable and specific RT-PCR procedure, based on fluorescence signal detection by hybridization probes. When the probes are in proximity, Förster resonance energy transfer proceeds between the probes and indicates their correct annealing to the amplicon cDNA in each PCR cycle. Sets of two primers and two fluorescent hybridization probes were designed as shown in the Table 1 for rat and mouse UCP2 (Růžička et al. 2005), UCP3, UCP4, and UCP5. A primer set for glyceraldehyde-3-phosphate dehydrogenase (*GAPDH*, a house-keeping gene) as well as primer and probe synthesis was provided by TIB MOLBIOL (Berlin, Germany).

Several essential criteria were kept for primer design in order to achieve the highest precision of mRNA quantification. Each PCR primer from a pair was designed to anneal to a different exon (corresponding to the unspliced mRNA molecule or to the gene sequence, where exons are separated by a long intron). This arrangement avoids any quantification of potential contaminating genomic DNA. PCR primers and hybridization probes were designed to hybridize the most variant part of the UCP sequence—the 5'-most—where various UCP isoforms differ (Ježek and Urbánková 2000). For example, in the case of rat UCP2 the amplicon spans 349 base pairs (i.e. bp 136–485). A 1-bp gap was usually left between adjacent hybridization probes (Table 1). We thus sacrificed to choose amplicons close to the 3' terminus, i.e. the way that also includes detection of mRNA that potentially could have been cut/damaged during isolation. In turn, our selected design for UCP3 and UCP5 covers all their splicing variants (Table 1). This is impossible to achieve with amplicons close to the 3' terminus.

Quantitative real-time RT-PCR

Routinely, 20–80 ng mRNA was used for real-time RT-PCR on a LightCycler (Roche) with 0.5 μ M primers and 0.2 μ M hybridization probes. Reverse transcription was performed (30 min at 55°C) followed by the reverse transcriptase inactivation for 30 s at 95°C, and then by 40 cycles of 2 s denaturation and annealing for 25 s at temperatures described in Table 1, and elongation for 25 s at 72°C. The $MgCl_2$ content was optimized for each set of primers and

probes (see Table 1). The absolute mRNA amounts, in picograms, were calculated from crossing points of each run. Calibrations were provided by seven order of magnitude-spanning dilution series of the PCR-amplified amplicons, starting from an initial concentration of 10 ng/ μ l. The calculated calibration slopes (Table 1) approached the predicted theoretical slope of 3.3, meaning that if two starting mRNA samples differed in content by one order of magnitude then equivalent amplified levels would be achieved 3.3 cycles apart. This is equivalent to doubling the amplicon amount in each single cycle.

A series of control experiments were performed for each sample. PCR product length was confirmed by electrophoresis on 1.5% agarose gels. To verify that the genomic DNA was not amplified and thus did not contribute to the quantification, the reverse transcription step was omitted in control runs; in such controls, no fluorescence was detected. The specificity of the primers and hybridization probes for mouse UCP2 was verified with the various tissue mRNA samples of UCP2 (–/–) mice (donated by B.B. Lowell, Harvard Univ., School of Medicine; Zhang et al. 2001), and no fluorescence was observed. Similarly, there was no cross-amplification between particular UCP isoforms when a PCR reaction was performed with a vector containing a cDNA for any other UCP isoform.

Results

mRNA levels for UCP2

We have confirmed the presence of UCP2 mRNA in all eight rat tissues studied (Fig. 1a). The absolute amount of UCP2 mRNA (in pg per 10 ng of total isolated mRNA) decreased in the order of spleen > heart > lung > WAT > brain > skeletal muscle > kidney > liver, spanning a 30-fold difference in UCP2 transcript content (Fig. 1a). Only in the rat spleen and lung were the UCP2 transcript levels of the same order of magnitude as the control GAPDH transcript levels. With the exception of the heart UCP2 mRNA, a similar pattern was found for mouse tissues (Fig. 2a). The heart UCP2 transcript level in mouse was up to 40-fold lower than in the mouse lung. In turn, the heart and lung UCP2 transcript levels were equivalent in the rat.

mRNA levels for UCP3

As expected (Boss et al. 1997; Vidal-Puig et al. 1997), we detected the highest UCP3 mRNA levels in rat and mouse skeletal muscle and intermediate levels in mouse heart (Fig. 1b, Fig. 2b), the latter being of the same order of magnitude as the UCP2 lung transcript levels. In contrast to the very high UCP2 mRNA levels found in the rat heart,

Table 1 Primer sets and fluorescent hybridization probes used for RT-PCR quantification of UCP mRNAs Primers (forward, f, reverse, r) and probes P_X and P_{LC} were designed as follows. X denotes the fluorescein fluorophore (donor); Red 640 is a Roche fluorophore (acceptor). The annealing temperatures were calculated by the synthesizing company (TIB MOLBIOL, Berlin, Germany)

	Sequence (5'→ 3') / excluded intron	Exon	Amplicon length MgCl ₂	Annealing temperature	Calibration Slope	Calibration Intercept
RAT						
UCP2	<i>f</i> GAGAGTCAAGGGCTAGCGC	exon 2				
	<i>r</i> GCTTCGACAGTGCTCTGGTA	exon 2	350 bp	58°C	- 3.543	- 20.84
	P _X TCAGAGCATGCAGGCATTGG X intron 1200 bp	exon 2/3				
	P _{LC} LC Red640-CCGCCTCCTGGCAGGTAGC p	exon 3	4 mM			
UCP3	<i>f</i> GTTGGACTTCAGCCATCAGAA	exon 1				
	<i>r</i> GTGGGTTGAGCACAGGTC	exon 3	418 bp	58°C	- 3.089	- 18.08
	P _X GAACGGACCACTCCAGCGTC X intron 1986 bp	exon 2/3				
	P _{LC} LC Red640-CCATCAGGATTCTGGCAGGCT p	exon 3	6 mM			
UCP4	<i>f</i> TGGCCGAGCTAGCAACC intron 3023 bp	exon 1/2				
	<i>r</i> CAGAGGGGATAATGTTCATCTTCA	exon 3	289 bp	58°C	- 3.061	- 17.13
	P _X CCATTTACAGACACGTAGTGTACTCTGGA X intron 2421 bp	exon 2/3				
	P _{LC} LC Rec 640-GTCGGATGGTCACCTACGAACAT p	exon 3	4 mM			
UCP5	<i>f</i> GATTGTAAGCGGACATCAG intron 4713 bp	exon 1/2				
	<i>r</i> GGTTGGCAATAGTAGATGAAATC see Footnote 1	exon 5	419 bp	58°C	- 3.170	- 18.15
	P _X CGCCATACACAAAAGGTTTCCA X	exon 2				
	P _{LC} LC Red640-TTCAGACCAGACATCTCATGGCTTAA p	exon 2	4 mM			
GAPDH	<i>f</i> AACTCCCTCAAGATTGTCAGCAA					
	<i>r</i> ATGTCAGATCCACAACGGATACA		316 bp	58°C	- 3.201	- 18.88
	P _X CAGTCTTCTGAGTGGCAGTGATGGCA X					
	P _{LC} LC Red705-ACTGTGGTCATGAGCCCTTCCACG p		4 mM			
MOUSE						
UCP2	<i>f</i> GAGAGTCAAGGGCTAGTGC	exon 2				
	<i>r</i> GCTTCGACAGTGCTCTGGTA	exon 3	349 bp	56°C	- 3.341	- 18.57
	P _X TCAGAGCATGCAGGCATCGG X intron 772 bp	exon 2/3				
	P _{LC} LC Red640-CCGCCTCCTGGCAGGTAGC p	exon 3	4 mM			
UCP3	<i>f</i> GTTTACTGACAACCTCCCCT intron 62 bp	exon 3/4				
	<i>r</i> CTCCTGAGCCACCATCT	exon 4	165 bp	56°C	- 3.363	- 18.96
	P _X AAGACCCGATACATGAACGC X	exon 4				
	P _{LC} LC Red640-CCCCTAGGCAGGTACCGCp	exon 4	5 mM			
UCP4	<i>f</i> GGACGAGCAAGTTCCTACTG	exon 1				
	<i>r</i> CCCTCCAATGACCGATTTTC see Footnote 2	exon 4	346 bp	56°C	- 3.470	- 16.05
	P _X CCATTTACAGACACGTAGTGTACTCTGGA X	exon 4				
	P _{LC} LC Red640-GTCGGATGGTCACCTATGAACATCTAC p	exon 4	6 mM			
UCP5	<i>f</i> CAGTGATTCATCAGAAAAGTTCCA intron 1/2 5054 bp	exon 1				
	<i>r</i> CCGTGTTTTAGTAAGATCCACAG intron 2/3 1543 bp	exon 3	133 bp	56°C	- 3.37	- 16.89
	P _X CGCCATACACAAAAGGTTTCCA X	exon 2				
	P _{LC} LC Red640-TTCAGACCAGACATCTCATGGCTTAA p	exon 2	5 mM			
GAPDH	<i>f</i> AATGGTGAAGGTTCGGTGTGA					
	<i>r</i> CTGGAAGATGGTGATGGGC		229 bp	56°C	- 3.364	- 21.57
	P _X GGCAAATTCAACGGCACAGTCAAG X					
	P _{LC} LC Red705-CCGAGAATGGGAAGCTTGTCATCAAC p		4 mM			

Footnote 1: intron 4/5 2083 bp, intron 3/4 2813, intron 2/3 1749 bp; Footnote 2: intron 1/2 2634 bp, intron 3/4 3809 bp, intron 2/3 2375 bp

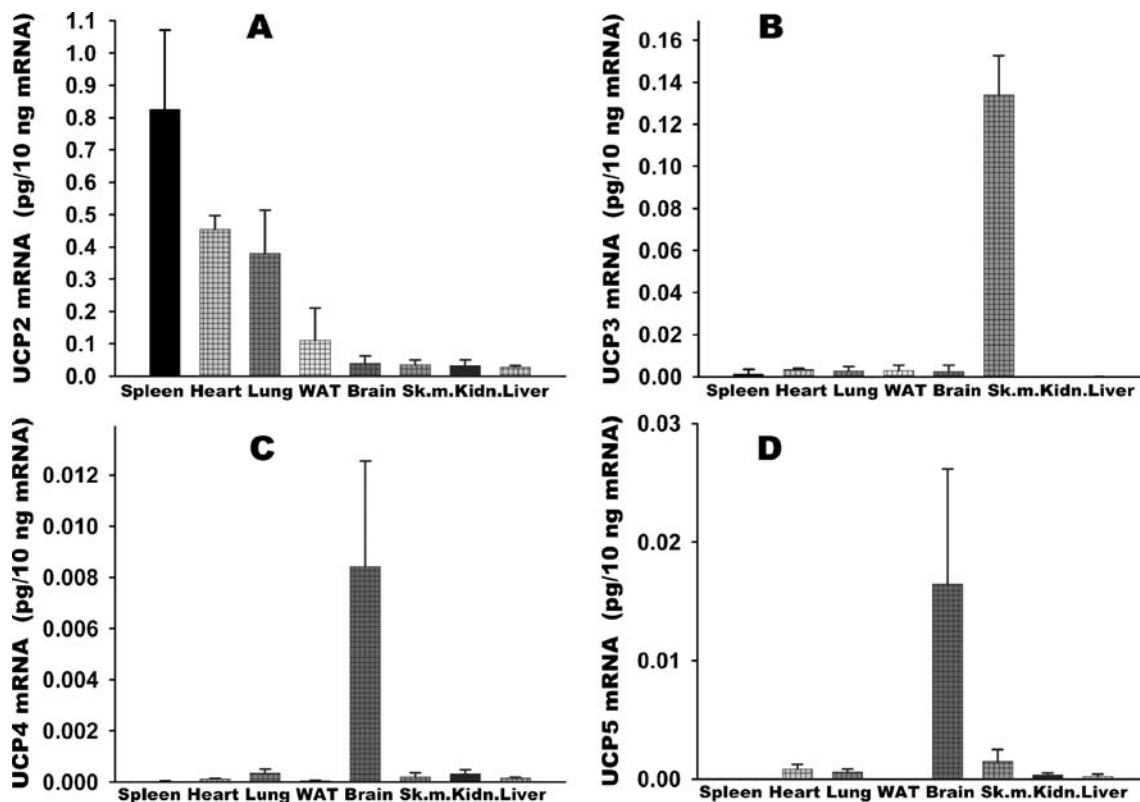


Fig. 1 Real-time RT-PCR quantification of UCP2 mRNA in rat tissues. The absolute amounts of transcripts (pg per 10 ng of total isolated mRNA) encoding UCP2 **a**, UCP3 **b**, UCP4 **c**, and UCP5

mRNA per day are plotted for selected rat tissues. Quantification, performed as described in Materials and methods, was derived according the calibrations with parameters listed in Table 1

the UCP3 mRNA was much less abundant. The other UCP3 transcript levels reached only $\sim 10^{-3}$ pg per 10 ng of total isolated mRNA with the exception of rat liver ($\sim 10^{-5}$) and rat kidney (not detectable, Fig. 1b). A similar pattern was found for mouse tissues, with the exception of higher levels of UCP3 transcript in the spleen and WAT (Fig. 2b). There was no compensatory increase in UCP3 transcript level in the heart of the UCP2 (-/-) mice (not shown).

mRNA levels for UCP4

The absolute mRNA levels of the UCP4 isoform in rat tissues were generally among the lowest determined (Fig. 1c). They were by up to three orders of magnitude lower than the UCP2 mRNA levels. As expected (Mao et al. 1999), the maximum UCP4 mRNA level was in the brain, but still two orders of magnitude lower than the UCP2 mRNA level. In turn, UCP4 transcript abundance in the rat brain (similarly for UCP5, see below) was similar to that of UCP2 mRNA in the mouse lung (Fig. 2c vs. Fig. 2a). The mouse skeletal muscle UCP4 transcript level exceeded that of UCP2. Similarly, mouse WAT contained nearly equivalent levels (~ 0.05 pg per 10 ng of total isolated mRNA) of UCP2, UCP3, and UCP4 transcripts. The UCP4 transcript level was not increased in the brain of

the UCP2 (-/-) mice compared with wild-type mice (not shown).

mRNA levels for UCP5

Similar to the rat UCP3 and UCP4 mRNAs, rat UCP5 mRNA was primarily expressed in a single tissue, namely brain. Whereas in the case of rat UCP3 such an apparent exclusivity was found in the skeletal muscle, in the case of rat UCP5 it was the brain (Fig. 1d). In other tissues the levels of UCP5 mRNA ($\sim 10^{-3}$ pg per 10 ng of total isolated mRNA) transcript levels of UCP5 were similar to the UCP3 levels. The rat UCP5 mRNA levels were still at least three-fold higher than those of UCP4. The tissue distribution of mouse UCP5 mRNA expression was somewhat more heterogeneous compared with the other UCPs, although UCP5 mRNA levels in brain were highest among the tested tissues (Fig. 2d). Notably, ~ 0.5 pg per 10 ng of total isolated mRNA was found for the UCP5 and UCP4 transcripts in the mouse brain, as well as for UCP2 mRNA in mouse lung and UCP3 mRNA in mouse skeletal muscle. The mouse heart UCP5 mRNA level was equivalent to that of UCP3. UCP5 mRNA in WAT and spleen was even more abundant than UCP3 mRNAs in these tissues and UCP2 mRNA in WAT. Although only at levels of ~ 0.05 pg per

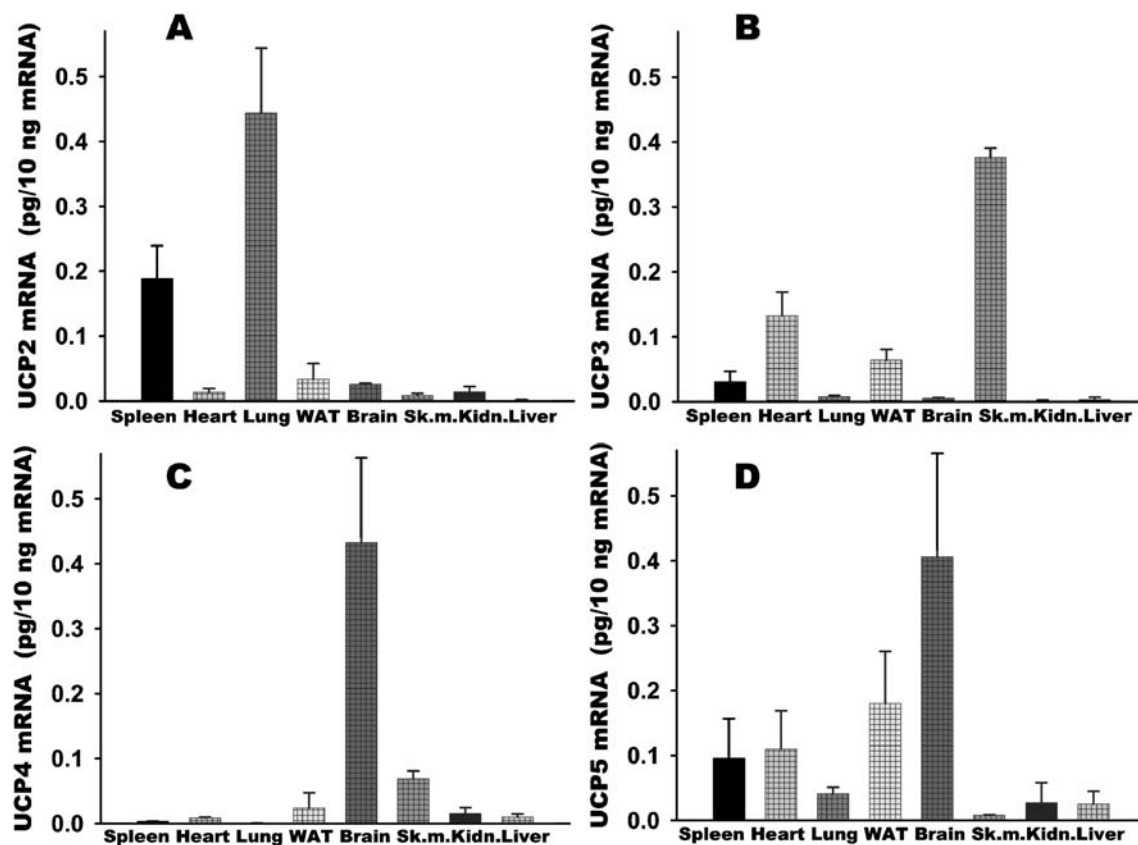


Fig. 2 Real-time RT-PCR quantification of UCP2 mRNA in mouse tissues. The absolute amounts of transcripts (pg per 10 ng of total isolated mRNA) encoding UCP2 **a**, UCP3 **b**, UCP4 **c**, and UCP5

mRNA per day are plotted for selected mouse tissues. Quantification, performed as described in Materials and methods, was derived according the calibrations with parameters listed in Table 1

10 ng of total isolated mRNA, UCP5 was the predominant isoform in the mouse liver and kidney. The UCP5 transcript was not elevated in the brain of UCP2 ($-/-$) mice.

Discussion

For the first time this work presents a unified quantification of UCP transcripts (with the exception of UCP1) in the heart, liver, kidney, brain, skeletal muscle, and WAT. The results clearly show that the tissue-specific expression pattern of individual isoforms is quite distinct between rat and mouse and that the levels of mouse UCP4 and UCP5 transcripts, previously considered to be very low, are in fact quite high. This finding sheds new light on previous studies in mice in which one isoform, UCP2 or UCP3, was ablated. Their reported interpretations might be yet inconclusive due to the possible expression of other UCP isoforms, if one considers the possibility of functional redundancy among UCPs.

The advantage of quantitative real-time PCR with properly designed primers and probes lies in the unsurpassed selectivity and resolution that are not achievable by northern blotting or “chip screening”. Thus we provide

reference data for the four UCP isoform transcript levels that span four to five orders of magnitude. The major question remains how the translation machinery deals with transcripts of such varying and distinct abundance. Is the resulting translation only 10,000-fold less frequent when the transcript is of 10^{-4} relative abundance? Alternatively, is there a threshold under which translation is nil for a very-low-abundance transcript? One could also speculate on the existence of a mechanism that upregulates the translation of low-abundance transcripts. Indeed, the observed disparity between the abundance of certain mRNAs and their corresponding protein products has been attributed to both translational down-regulation (Pecqueur et al. 2001; Hurtaud et al. 2006) and up-regulation (Hurtaud et al. 2007).

We have chosen a reference unit that is quite versatile and has practical implications, namely the unit of picograms of a given transcript per 10 ng of total isolated mRNA. One unit is close to the expected average transcription of 10,000 genes if all genes were transcribed equivalently. Only the level of the UCP2 transcript in the rat spleen approached one such unit. The selected reference gene, *GAPDH*, was transcribed in different tissues at levels between 1 and 10 pg per 10 ng of total isolated mRNA, corresponding to 0.01% to 0.1% of average gene represen-

tation (mRNA abundance). The finding that UCP2 transcript abundance was highest in the spleen points to important physiological role of UCP2 in macrophages (Arsenijevic et al. 2000; Giardina et al. 2008) and other white blood cell types, resident in the spleen. Similarly, the second highest UCP2 transcript amount, found in the rat and mouse lung, may reflect its predominating expression in the alveolar macrophages.

Attempting at least to find the order of magnitude proportionality between the measured levels of UCP mRNAs and their corresponding protein products, we can compare data for mouse spleen. These data show that UCP2 accounts for ~0.03% of all mitochondrial proteins (Pecqueur et al. 2001). Compare this to our finding of 0.002% for UCP2 transcript abundance (Fig. 2a). Considering on average 10,000 transcribed genes as 100%, these data would match only, if approximately each tenth transcribed protein in general was mitochondrial. The reported mouse lung UCP2 protein level (~0.002% of rat mitochondrial proteins, Pecqueur et al. 2001) seems to correlate with a rather high estimated transcript abundance of 0.004% (Fig. 2a). Also, our [³H]GTP binding study reflecting UCP2 protein amounts (Žáčková et al. 2003) correlated better with the rat UCP2 transcript quantification (Fig. 1a), indicating rather high amounts of UCP2 protein in rat lung mitochondria, and 10-fold lower levels in rat liver mitochondria (Žáčková et al. 2003). Indeed, the UCP2 mRNA was one order of magnitude greater in lung than in liver (Fig. 1a).

With the precision of calibrated real-time RT-PCR, we can claim that when no amplification proceeds within a sample there is definitively no transcript present, unless it exists in the range of attograms per 10 ng of total isolated mRNA. With such sensitivity, we identified UCP5 and UCP4 transcripts in all tested rat tissues, and we confirmed previous findings of UCP5 mRNA in mouse liver, lung, kidney, and spleen (Sanchis et al. 1998), heart (Kim-Han et al. 2001; Sanchis et al. 1998; Yu et al. 2000), and skeletal muscle (Lengacher et al. 2004; Sanchis et al. 1998; Yu et al. 2000). In the mouse these transcripts levels were very high (0.1 pg per 10 ng of total isolated mRNA, Fig. 2d). Also surprising was the rather high UCP4 mRNA level in mouse skeletal muscle (up to 0.1 pg per 10 ng of total isolated mRNA), being only five times lower than the UCP4 transcript level in mouse brain (Fig. 2d).

Patterns of the four studied UCP isoforms are remarkable for the heart and brain. In the rat heart, UCP2 mRNA was present at up to 0.5 units (i.e. pg per 10 ng of total isolated mRNA, the second highest level measured in our tissue set), exceeding by the two to three orders of magnitude the levels of UCP3, UCP4, and UCP5 transcripts. In turn, among mouse UCP mRNAs, UCP3 and UCP5 mRNAs were the most abundant and nearly

equivalent, whereas UCP2 mRNA was 10-fold less abundant. For reason unknown, UCP2 seems to have been phylogenetically selected for its role in the rat heart, and likewise for UCP3 and UCP5 in the mouse heart. This finding puts into context the previous striking reports demonstrating the importance of UCP2 function in the rat heart (Bo et al. 2008; McLeod et al. 2005).

In the rat brain, the predominant rat UCP2 transcript and roughly half-abundant UCP5 transcript exceeded 10-fold the UCP4 mRNA levels, whereas, on the contrary, in the mouse brain the UCP4 transcript and the equally abundant UCP5 transcript outnumbered UCP2 mRNA by 10-fold. In conclusion, the tissue distribution of UCP isoform mRNAs differs between rat and mouse. As such, researchers must heed caution when extrapolating the findings/conclusions for one of these rodent species onto the other and when reporting on studies of single-gene knockout mice.

Acknowledgement The project was supported by grants of the Grant Agency of the Czech Republic (No. 303/07/0105), the Internal Grant Agency of the Academy of Sciences of the Czech Republic (No. A500110701); the Czech Ministry of Education (No. 1P05ME794) and the research project AV0Z50110509. We gratefully acknowledge the excellent technical assistance of Dr. M. Růžicka with regard to tissue removal.

References

- Adams AE, Carroll AM, Fallon PG, Porter RK (2008a) *Biochim Biophys Acta* 1777:772–776
- Adams AE, Hanrahan O, Nolan DN, Voorheis HP, Fallon P, Porter RK (2008b) *Biochim Biophys Acta* 1777:115–117
- Affourtit C, Crichton PG, Parker N, Brand MD (2007) *Novartis Found Symp* 287:70–80
- Arsenijevic D, Onuma H, Pecqueur C, Raimbault S, Manning BS, Miroux B, Couplan E, Alves-Guerra MC, Goubern M, Surwit R, Bouillaud F, Richard D, Collins S, Ricquier D (2000) *Nat Genet* 26:435–439
- Beck V, Jabůrek M, Demina T, Rupprecht A, Porter RK, Ježek P, Pohl EE (2007) *FASEB J* 21:1137–1144
- Bo H, Jiang N, Ma G, Qu J, Zhang G, Cao D, Wen L, Liu S, Ji LL, Zhang Y (2008) *Free Radic Biol Med* 44:1373–1381
- Boss O, Samec S, Paoloni-Giacobino A, Rossier C, Dulloo A, Seydoux J, Muzzin P, Giacobino JP (1997) *FEBS Lett* 408:39–42
- Cannon B, Shabalina IG, Kramarova TV, Petrovic N, Nedergaard J (2006) *Biochim Biophys Acta* 1757:449–458
- Carroll AM, Haines LR, Pearson TW, Fallon PG, Walsh CM, Brennan CM, Breen EP, Porter RK (2005) *J Biol Chem* 280:15534–15543
- Chan SL, Liu D, Kyriazis GA, Bagsiyao P, Ouyang X, Mattson MP (2006) *J Biol Chem* 281:37391–37403
- Chomezynski P, Sacchi N (1987) *Anal Biochem* 162:156–159
- Dlasková A, Hlavatá L, Ježek P (2008a) *Int J Biochem Cell Biol* 40:2098–2109
- Dlasková A, Hlavatá L, Ježek J, Ježek P (2008b) *Int J Biochem Cell Biol* 40:1792–1805
- Dlasková A, Špaček T, Škobisová E, Šantorová J, Ježek P (2006) *Biochim Biophys Acta* 1757:467–473
- Esteves TC, Brand MD (2005) *Biochim Biophys Acta* 1709:35–44

- Fleury C, Neverova M, Collins S, Raimbault S, Champigny O, Lévi-Meyrueis C, Bouillaud F, Seldin MF, Surwit RS, Ricquier D, Warden CH (1997) *Nat Genet* 15:269–272
- Giardina TM, Steer JH, Lo SZ, Joyce DA (2008) *Biochim Biophys Acta* 1777:118–129
- Gimeno RE, Dembski M, Weng X, Shyjan AW, Gimeno CJ, Iris F, Ellis SJ, Deng N, Woolf EA, Tartaglia LA (1997) *Diabetes* 46:900–906
- Hanák P, Ježek P (2001) *FEBS Lett* 495:137–141
- Ho PW, Chu AC, Kwok KH, Kung MH, Ramsden DB, Ho SL (2006) *J Neurosci Res* 84:1358–1366
- Ho PW, Chan DY, Kwok KH, Chu AC, Ho JW, Kung MH, Ho SL (2005) *J Neurosci Res* 81:261–268
- Hurtaud C, Gelly C, Bouillaud F, Lévi-Meyrueis C (2006) *Cell Mol Life Sci* 63:1780–1789
- Hurtaud C, Gelly C, Chen Z, Lévi-Meyrueis C, Bouillaud F (2007) *Cell Mol Life Sci* 64:1853–1860
- Jabůrek M, Miyamoto S, Di Mascio P, Garlid KD, Ježek P (2004) *J Biol Chem* 279:53097–53102
- Ježek P, Hlavatá L (2005) *Int J Biochem Cell Biol* 37:2478–2503
- Ježek P, Ježek J (2003) *FEBS Lett* 534:15–25
- Ježek P, Urbánková E (2000) *IUBMB Life* 49:63–70
- Ježek P, Žáčková M, Růžička M, Škobisová E, Jabůrek M (2004) *Physiol Res* 53:S199–S211
- Kim-Han JS, Reichert SA, Quick KL, Dugan LL (2001) *J Neurochem* 79:658–668
- Klingenspor M, Fromme T, Hughes DA Jr, Manzke L, Polymeropoulos E, Riemann T, Trzcionka M, Hirschberg V, Jastroch M (2008) *Biochim Biophys Acta* 1777:637–641
- Lengacher S, Magistretti PJ, Pellerin LJ (2004) *J Cereb Blood Flow Metab* 24:780–788
- Liu D, Chan SL, de Souza-Pinto NC, Slevin JR, Wersto RP, Zhan M, Mustafa K, de Cabo R, Mattson MP (2006) *Neuromolecular Med* 8:389–414
- Mao W, Yu XX, Zhong A, Li W, Brush J, Sherwood SW, Adams SH, Pan G (1999) *FEBS Lett* 443:326–330
- McLeod CJ, Aziz A, Hoyt RF Jr, McCoy JP Jr, Sack MM (2005) *J Biol Chem* 280:33470–33476
- Mori S, Yoshizuka N, Takizawa M, Takema Y, Murase T, Tokimitsu I, Saito M (2008) *J Invest Dermatol* 128:1894–1900
- Nakase T, Yoshida Y, Nagata K (2007) *Neuropathology* 27:442–447
- Naudí A, Caro P, Jové M, Gómez J, Boada J, Ayala V, Portero-Otín M, Barja G, Pamplona R (2007) *Rejuvenation Res* 10:473–484
- Pecqueur C, Alves-Guerra M-C, Gelly C, Lévi-Meyrueis C, Couplan E, Collins S, Ricquier D, Bouillaud F, Miroux B (2001) *J Biol Chem* 276:8705–8712
- Růžička M, Škobisová E, Dlasková A, Šantorová J, Smolková K, Špaček T, Žáčková M, Modrianský M, Ježek P (2005) *Int J Biochem Cell Biol* 37:809–821
- Sale MM, Hsu FC, Palmer ND, Gordon CJ, Keene KL, Borgerink HM, Sharma AJ, Bergman RN, Taylor KD, Saad MF, Norris JM (2007) *BMC Endocr Disord* 30:7–1
- Sanchis D, Fleury C, Chomiki N, Goubem M, Huang Q, Neverova M, Grégoire F, Easlick J, Raimbault S, Lévi-Meyrueis C, Miroux B, Collins S, Seldin M, Richard D, Warden C, Bouillaud F, Ricquier D (1998) *J Biol Chem* 273:34611–34615
- Vidal-Puig A, Solanes G, Grujic D, Flier JS, Lowell BB (1997) *Biochem. Biophys. Res. Commun* 235:79–82
- Yu XX, Mao W, Zhong A, Schow P, Brush J, Sherwood SW, Adams SH, Pan G (2000) *FASEB J* 14:1611–1618
- Zhang CY, Baffy G, Perret P, Krauss S, Peroni O, Grujic D, Hagen T, Vidal-Puig AJ, Boss O, Kim YB, Zheng XX, Wheeler MB, Shulman GI, Chan CB, Lowell BB (2001) *Cell* 105:745–755
- Zhang M, Wang B, Ni YH, Liu F, Fei L, Pan XQ, Guo M, Chen RH, Guo XR (2006) *Life Sci* 79:1428–1435
- Žáčková M, Škobisová E, Urbánková E, Ježek P (2003) *J Biol Chem* 278:20761–20769